The Life and Death of Stylolites: stylolite roughness as indicator for the duration and amount of dissolution

Leehee Laronne Ben-Itzhak, Einat Aharonov, Renaud Toussaint, Amir Sagy

The Life and Death of Stylolites: stylolite roughness as indicator for the duration and amount of dissolution

Laronne Ben-Itzhak Leehee[1,2], Aharonov Einat[2], Toussaint Renaud[3] and Sagy Amir[4]

[1] Weizmann Institute of Science, P.O. Box 26, Rehovot 76100, Israel.
[2] The Hebrew University of Jerusalem, The Institute of Earth Sciences, Givat Ram, Jerusalem, 91904, Israel.
[3] Institut de Physique du Globe de Strasbourg, CNRS, University of Strasbourg, 5 rue Descartes, F-67084 11 Strasbourg Cedex, France.
[4] Geological Survey of Israel, 30 Malkhe Israel St., Jerusalem 95501, Israel.

Abstract

Stylolites are rough surfaces formed by localized dissolution, mostly in carbonates and sandstones. They often account for a large degree of dissolution, and their impact on porosity and permeability is well recognized. Understanding their formation mechanism can advance our ability to predict their occurrence and effect on flow, which has appreciable geological and economical implications. Still, many fundamental issues concerning their structure and evolution are still unresolved. This manuscript studies the roughening of long parallel stylolites, which are one of three types of stylolite populations identified by us in a separate paper. Here we report measurements of stylolite surface roughness at a scale larger than ever measured before (10^{-2}-10^{1}m). Measurements were performed using ground-based-LIDAR on 6 naturally-exposed surfaces of >km long stylolites in Northern Israel. The outcome of these measurements is a topography model of the surfaces, on which different techniques for calculating their roughness characteristics were used. Our results show that up to scales of ~10cm, the average deviation of the surfaces from a planar surface is related to the scale by a power-law with an exponent H. The surfaces are thus defined as self-affine only up to ~10cm with H~0.7. Above this scale H decreases almost to zero. This observed upper-bound of self-affine roughness measured here for the first time has been predicted by theory [1, 2, 2bis]. Our measurements support these theoretical models and together with them present a scenario in which stylolites evolve from preferential dissolution along an existing surface that was initially smooth and progressively roughened with time. Such a mechanism of stylolites growth is different from previously suggested mechanisms for other classes of stylolite which might propagate sideways from an initial defect. Based on the theoretical

roughening model that we adopted, the upper limit to fractality for this class of stylolites may be used as a measure of the amount of dissolution on stylolites. Indeed, the amount of dissolution of the stylolites in our field site which we calculated from the upper limit to fractality is comparable to our estimates of dissolution from two additional independent techniques.

Keywords

Stylolites, Surface Roughening, Pressure Solution, Porosity, LIDAR

1 Introduction

Stylolites are rough dissolution surfaces abundantly found in carbonates and sandstones [3-7] . They are lined by insoluble material (mainly clay minerals, oxides, and organic matter) which accumulates as the more soluble rock constituents dissolved [5, 6]. They are characterized by anomalous porosity and permeability with respect to the host rock, and thus play a crucial role in determining both the deformation and permeability of rocks. In spite of their importance and decades of research, their formation is still not well understood. Specifically, the propagation and development of stylolites, as well as the controls on their lateral extent and teeth-amplitude is of interest.

In [8] we showed that sedimentary stylolites usually appear not as isolated features, but in three main types of "populations" or "stylolite networks": **isolated**, self-similar stylolites, which have clear edges; networks of **long bedding-parallel stylolites** with uniform dissolution along the seam; and **networks of interconnected stylolites** with or without fractures. The evolution of the various populations was successfully modeled in [8] assuming that the initial distribution of heterogeneities (such as clay) in the rock

determines which kind of network will form and the lateral extent of the stylolites in the network.

In many examples stylolite teeth amplitude displays multiscale roughness characteristics that can be evaluated as statistically self-affine [1, 9-11]. A self-affine 1-D profile remains unchanged under the scaling transformation $\delta x \to \lambda \delta x$, $\delta z \to \lambda^H \delta z$ [12]. For 2-D surfaces, this self-affinity property can be described for sets of 1-D parallel profiles extracted from the surface. The roughness characteristics of a surface, such as whether it is self-affine or not, or the value of its Hurst exponent H which characterizes its self-affinity, and whether this parameter H varies with scale and the scale ranges, can give physical indications on the formation mechanisms when confronted with theory. This has been claimed with regard to stylolites by [2bis, 10, 11, 13, 14]. They found two self-affine regimes for scales smaller and larger than ~1.1mm and connected this to two competing mechanisms driving dissolution: surface energy for smaller scales and elastic strain energy for the larger scales. The largest surfaces analyzed by [2bis, 10, 11, 13, 14] were ~10cm long. Since stylolites are often larger than 10cm ([15, 16] reported 8.5-m-long stylolites in chalk and in [8] we describe the >1km-long stylolites which are measured in this current paper), studying roughness of stylolites on larger scales could lead to further insight on their formation process.

The present paper focuses on field measurements, characterization, and modeling of the formation and evolution of one of the three stylolite populations mentioned above: the long bedding-parallel stylolites. Roughness measurements were performed on long stylolite surfaces in the "Blanche cliff", Northern Israel. Our very unique long scale measurements (10^{-2}-10^{1}m) show that stylolite roughness is scale-dependent up to ~10^{-1} m, where a clear cutoff to this dependence appears. To model and explain these unique observations of the statistical properties over many scales we use growth models of stylolites roughening from an initial flat surface [1, 2, 2bis, 10, 11, 14]. The similarity between these models and the field measurements supports our claim that long parallel stylolites form on existing, very long (practically infinite) bedding-parallel surfaces undergoing preferential dissolution (e.g., surfaces of higher clay content). This is in

contrast to isolated, single stylolites which have been suggested to propagate sideways from an initial defect (e.g. [17]).

We explain in this manuscript how these models can be used to calculate the amount of dissolution on stylolites. The amount of dissolution is calculated for stylolites in the Blanche site, and is compared to values obtained by two other methods. We discuss when roughness measurements can be used as a method for calculation of dissolution amount on stylolites.

2 Field observations: Large scale roughness measurements of stylolites

Out of several field sites we identified in [8] as belonging to the long-bedding parallel stylolite population class, we focus here on the "Blanche" cliff of the Ein El-Assad Formation (Albian) exposed in Northern Israel (Figure 1), due to its unique exposure length (>1km), and its well developed stylolites (teeth amplitude on the scale of cm). It is a roughly 50m thick shallow inner-platform biomicritic limestone formation, with very low porosity, that dips gently to the west [18]. The bedding-parallel stylolites can be traced through the entire outcrop (>1km), and most likely continue beyond the exposure. Such a tracing length for stylolites is remarkable, and is observed for the first time. It has implications for understanding scales of permeability units and their structural continuity. Several large oil-reservoirs of the same geological age also contain stylolites which are claimed to highly affect porosity [19]. Detailed field-work conducted in this site [8] showed that the stylolites are similarly developed along their whole length and keep their spacing. The stylolites were suggested to form on pre-existing layers, possibly with higher clay content compared to the surrounding rock.

This paper studies stylolitic roughness as a recorder of stylolitic development. Thus roughness of exposed stylolite surfaces in the Blanche (such as in Figure 1b) was measured, using Ground-based LIDAR. We used the Leica HDS3000 Laser scanner

which provides resolution of ~ 3 mm when a target is scanned from a distance of 20-30 m. A single scan can provide a cloud with millions of points that may be interpolated to generate a topographic map or hundreds of profiles (Figure 2). Thus, the technique allows a statistical approach when calculating roughness. The scan data are rotated so that the mean surface is parallel to the x-y plane. The cloud of points is then interpolated to an x-y-z grid, in which the topography is the value of the z-coordinate. Four surfaces were scanned *in-situ* and two scans were performed on "rockfalls" – m-size blocks that detached from the cliff. Surfaces with minimum erosion were picked for scanning. The measured surfaces range in size from 2.1*0.2 m^2 to 9.3*3.0 m^2 (see Table 1). The obtained measurements of stylolite surface roughness range in scale between 10^{-2}-10^{1}m, larger than ever measured before (so far the highest resolution measurements reported in the literature were done up to maximum scales around 10^{-1}m, as e.g. in [1]). The scanned surfaces have cm-scale teeth amplitude, are symmetric with respect to the surface average plane (in the z-direction) and demonstrate no anisotropy (similar roughness characteristics in the x and y directions), as was found by performing the analyses explained below on length-parallel and width-parallel profiles. Results are presented for length-parallel profiles (Figure 3 and Table 1) so that larger scales can be studied.

2.1 Characterization of roughness

Characterization of rough surfaces depends on the scale of measurement. One common method is to measure the surface width (in the z-direction) as a function of the window at which the measurement is made (l). Maximum width ($w_\infty(l)$ according to [20]) or average width $w(l)$ are commonly used, with the latter calculated by the **standard deviation (STD) of its height from the average surface height**. STD is defined by the Root Mean Square method (after [21]):

$$(1) \qquad w(l) \equiv \frac{1}{l}\sqrt{\sum_{i=1}^{l}(h(i)-\bar{h})^2}$$

The smallest possible value for l (the smallest window for measuring width) is the distance between two data points. In our case, it is the distance between two points on the interpolated x-y grid (either 2 or 3 mm, for each surface). The largest value for l is the

length of the surface. When a surface is self-affine, w and *l* are related by a power law with an exponent H, termed the Hurst exponent [21]. This exponent can be derived using other common methods for surface characterization, such as power spectral density (PSD) as performed on stylolites e.g. by Renard et al., [10] and on fault surfaces e.g. by Sagy and Brodsky [22]. Power spectral density measures the strength of the sinusoidal components of the topography over a range of wavelengths by performing a Fourier decomposition. We average the 1-D spectra of hundreds of profiles in the x and in the y direction for each surface in order to arrive at a spectral estimate with minimal variance.

Figure 3a shows results of the average width of the six stylolite surfaces, w, as a function of measurement window, *l*, calculated following equation (1). The six surfaces show very similar behavior with two scaling regimes: above and below l= 10 ±3 cm. Up to this value of *l* the surfaces are self-affine with Hurst exponents of 0.67 ±0.10 (the error is the standard deviation of H of the six measured surfaces). For larger values of *l* the Hurst exponent is not constant and decreases to almost zero (H=0.10 ±0.06 for scales above ~1m). Therefore we identify an upper cutoff to the self-affine behavior of these stylolite surfaces: they appear rough on small scales, but at large enough scales (i.e. viewed from far enough away) they are smooth. The PSD analyses presented in Figure 3b, as well as an additional analysis using the wavelet technique (Determination of the Hurst exponent by use of wavelet transforms, Simonsen, I; Hansen, A; Nes, OM, PHYSICAL REVIEW E, 58, 3, 2779-2787, DOI: 10.1103/PhysRevE.58.2779, 1998) both provided similar values of H as the ones calculated by RMS, as evident in Table 1.

3 Existing models of stylolite roughening from an initially flat surface

Our roughness measurements can be compared to predictions offered by existing roughening models which assume an initially flat surface and predict how stylolite roughness will develop with time [1, 2, 10, 11, 14]. Rolland et al. [2bis] or Schmittbuhl et

al. [11] offers an analytic formulation and solution to the temporal and spatial evolution of the surface height, h, with a governing equation:

$$(2) \qquad \frac{\partial h}{\partial t}(x) = h_{xx}(x) - \frac{a}{L}\int dx' \frac{h_x(x')}{x - x'} + \eta(x, h)$$

Three terms appear on the right side of equation (2) and these control the roughening processes (from left to right): a surface energy term, an elastic strain energy term, and a term representing the spatial solubility heterogeneity. Here, *a* and L represent respectively a characteristic grain scale and a scale derived from the far field stress components, the elastic moduli, and the surface tension. In this equation, x, t and h are reduced dimensionless quantities, with a unit length, and a unit time set by a/v, with v an average dissolution speed.

Numerical solutions to the evolution of stylolite roughness from an initial flat surface are presented by [1, 2, 10, 14]. They simulate two granular rock bodies pressed together with a predefined fluid-filled flat interface on which dissolution occurs. The solubility of the rock is not homogeneous and this "quenched noise" is introduced by assigning a lower dissolution rate constant to a certain fraction of the particles. This is seen in Figure 4 (from Ebner et al., [14]): darker, less soluble grains get pinned and stuck in the interface as dissolution evolves. The pressure solution process is discretized in steps of dissolution of entire particles, following a linear rate law (see equation (1) in [14]). According to this rate law, the dissolution velocity depends on the local elastic and surface energies and on the local deviation of normal stress from its average value on the surface.

Both the analytical and numerical models described above [1, 2, 10, 11, 14] assume **three controlling processes**: The first is that the system has pinned noise, provided by the heterogeneous solubility of the rock, which is the main drive for roughening. The second is that the process has long-range interactions, here provided by elastic surface forces which are increased by the surface misalignment on the normal to the principal far field stress axis. The third process is diffusion and smoothing, here provided by surface energies, which cause smoothing of the interface. The models presented above quantify

stylolite roughness evolution by evolving Fourier or wavelet transforms, or by the evolution of surface average width, w (equation 1) as a function of **time, t,** and of the **sampling size, *l***.

The evolution of stylolite surface width with time and sampling size according to these models is illustrated schematically in Figure 5 (here the maximum width, $w_\infty(t,l)$, is shown since average width is harder to show visually; both quantities evolve in a similar manner). At any given time there is a critical sampling size, above which w_∞ is constant. For example, in Figure 5 this critical size at time t_3 is l_2. This behavior of surface evolution belongs to a universality class of surface growth models of the Family Viscek type, i.e. where the surface dynamics shows a Family Vicsek scaling [23], on which much has been written (e.g.: [21]). Other phenomena such as flame fronts, viscous fingering, electrochemical crystals and the dynamics of bug colonies obey such scaling. All these surfaces develop in a similar manner, thus the parameters used to describe stylolite roughening are conventional parameters.

Mathematically, all functions $w(l,t)$ can be collapsed on a Family Vicsek scaling form as:

(3) $$w(l,t) \sim l^H f\left(\frac{l}{\chi}\right);$$

where $f(u)$ is a universal scaling function, and χ, is a critical sampling size which is a simple function of t. The scaling function has the following asymptotic behaviors:

$f(u) = const \quad For \quad u << 1$ and: $f(u) = u^{-H} \quad For \quad u >> 1$, which reflects the fact that:

(4) $$w(l,t) \sim l^H \quad \rightarrow For \quad l < \chi$$

which means that for measurement samples smaller than a size of the correlation length χ, the width, w, is a power law of the sampling size, *l*, only, and is independent of time. The scaling exponent, H is the Hurst exponent. The width in these small windows will never grow anymore, even though the surface keeps on evolving as a whole, since these small wavelengths have saturated.

In contrast, for measurement windows larger than χ:

(5) $$w(l,t) \sim l^H \left(\frac{l}{\chi}\right)^{-H} = \chi^H = t^{\frac{H}{Z}} \quad \rightarrow For \quad l > \chi$$

the width, w, is independent of the measurement scale, l. It is constant no matter how large the sampling window is, but instead it grows as a power law of time.

The conceptual evolution of w(t,l) for several times according to the models described above is plotted schematically on a log-log scale in Figure 6. For a given time, t_i, w(l) increases as a power-law up to a value of $l \approx \chi$ above which w(l) becomes constant. This critical sampling size, χ is termed the "correlation length", and can be viewed as a characteristic distance between two points on the surface that are influenced by one another. χ increases as a power-law with time following

(6) $$\chi \sim t^{1/z}$$

where "z" is called *the dynamic exponent (or growth exponent)*. The correlation length continues to grow according to (6) unless χ reaches the system size, at which time it stops growing. In the case of stylolite growth models, z can be evaluated from time-dependant models. In the model of [14] z≈1.2 and similar or slightly lower values are given by [11, 24].

Equations (4) and (5) are scaling equations. In order to relate w concretely to other length scales, we normalize these equations by a - a characteristic size of the system, which might be related to an average or a characteristic grain diameter scale, at which the out of plane and in plane amplitudes are of the same order, i.e. $w(l) \approx l$. This scale characterizes the prefactor of scaling laws for self affine functions, and is also called the topothesy [25-27].

3.1 Amount of dissolution

We next wish to infer the unknown amount of dissolution, A, that occurred on the stylolite (in meters), from the width measured in models or in the field. This may be done

if we assume the dissolution rate (v, in m/s) was constant, so that A=vt, where t represents the time during which dissolution has been active (between the start of the roughening up to when dissolution stopped).

Therefore, with:

(6) $\frac{w}{a}=\left(\frac{l}{a}\right)^{H} \rightarrow For \quad l<\chi$; and by plugging t=A/v into equation (3) one can obtain:

(7) $\frac{w(l,t)}{a}=\left(\frac{vt}{a}\right)^{\frac{H}{Z}}=\left(\frac{A}{a}\right)^{\frac{H}{Z}} \rightarrow For \quad l>\chi$

The relationship between χ and A is then:

(8) $\left(\frac{\chi}{a}\right)=\left(\frac{A}{a}\right)^{\frac{1}{Z}}$

Thus in order to calculate how much dissolution A occurred on stylolites one basically needs to have roughness measurements on a scale larger than χ, so as to capture accurately χ and $w(\chi)$.

4 Implementation of the roughening models to the Blanche stylolites

The measured roughness characteristics (section 2) are similar to those of the models (section 3) in the fact that both demonstrate self-affine behavior up to a certain length and a crossover transition towards a very low roughness exponent above that length. The roughness exponent in the theoretical model equals zero for $l>>\chi$. Our measurements show a value for H which is very low and close to zero (0.10 ±0.06, Table 1), as expected for surfaces following a complete Family Vicsek scaling. We can thus consider the measured cutoff as the correlation length of the Blanche stylolites with $\chi \approx 10cm$. Our system size L is >1km, which is the observable length of the stylolites, so $L>>\chi$ and we can use χ or $w(\chi)$ to calculate the average amount of dissolution that occurred on the Blanche stylolites

By plugging into equation (6) the values of χ, $w(\chi)$ and H of the self-affine part of the plot for each surface we can calculate the characteristic size, *a*:

$$\frac{w(\chi)}{a}=\left(\frac{\chi}{a}\right)^{H} \quad \rightarrow \quad a=\left(\frac{w(\chi)}{\chi^{H}}\right)^{\frac{1}{1-H}}$$

We find that *a* on average is ~20μm (see Table 1). We can then use either equation (7) or (8) to calculate the amount of dissolution, A:

$$A=\left(\frac{w(\chi)}{a}\right)^{\frac{Z}{H}} a$$

$$A=\left(\frac{\chi}{a}\right)^{Z} a$$

With the range of literature values for the dynamic exponent z, we find: for z=1.2, **A≈70cm** (this is for the average value of z in Koehn et al., [2]); for a slightly lower value of z=1.0, **A=10cm**. The detailed results of these calculations (Table 1) demonstrate that the variability of A from one surface to another is much smaller than the sensitivity of A to the selected value of z. E.g. for z=1.2, A varies between 50 and 100 cm, whereas A is 5-10 times higher for z=1.2 compared to z=1.0 for a given surface. With an average spacing, $\bar{d}$, of ~30cm between stylolites in the Blanche cliff this translates to between 10cm/(10+30)cm=**25%** and 70cm/(70+30)cm=**70%** strain.

An alternative method to calculate A is by a simplified **mass-balance**. Here we assume that (1) stylolites are the only source for cement, and (2) we have a closed system, meaning that material dissolving on stylolites precipitates in the available porosity and that porosity at the end of the process is close to zero. Several thin-sections that we prepared and studied, taken from the stylolites and up to several cm away from them show no porosity at this scale and thus support our assumption of zero porosity around the stylolites. We estimate from these thin section that the initial porosity, φ, is in the range of 0.2-0.3. Thus, we basically assume that initial porosity was completely shut by cement originating from dissolution on the stylolites. Using $\bar{d}$=30cm we can calculate A:

$$A = \frac{\phi \bar{d}}{1-\phi} \approx \frac{0.2 * 30cm}{(1-0.2)} = 7.5cm \quad (or \quad 12cm \quad for \quad \phi = 0.3)$$

This translates to between **20%** and **30%** strain, and is comparable to our lower roughness-based estimates (with z=1.0).

A third independent method we used to evaluate the amount of dissolution is by **maximum amplitude of stylolites** (peak-to-peak) measured in 2D in the field, assuming it is a minimum estimate to the amount of dissolution. A_{max} was also used by Schmittbuhl et al., [20] who defined it as w_∞. Our field-measurements, which are described in detail by [8], show A_{max}≈4cm for one stylolite and A_{max}≈10cm for another. These values are also comparable to the lower estimates of dissolution of the roughness-based method. All three independent methods give similar estimates within an order of magnitude, which we interpret as a good sign of their validity.

5 Discussion

We have demonstrated in this paper how models of stylolite roughening from an initial flat surface can be used to explain measurements that were performed on long parallel stylolites in the Blanche cliff, Northern Israel. Our roughness analysis on surfaces of several different stylolites from this site showed that the stylolites are self-affine below ~10cm with H≈0.7. This upper cutoff to fractality was consistent among several surfaces from different stylolites and we correlate it with the model-predicted cutoff to fractality, also termed the "correlation length", χ. Above this length, measured roughness decreased significantly, as quantified by the decrease in H (to ~0.1 or even lower).

5.1 The life and death of the Blanche stylolites

The conformity between the roughening models and our measurements agrees with a picture of dissolution occurring preferentially along a surface. This surface was initially

smooth and progressively roughened with time. Had stylolitization in the Blanche continued for a long enough time we would have expected to see a self-affine behavior on all scales. The Blanche stylolites are not self-affine in the large scale, which implies that the stylolitization process had stopped at some stage. The reason for termination of the stylolitization process could be related to porosity destruction resulting in no place available for precipitation, an option which is supported by the mass balance calculations for A and by the thin-section observations, as explained above. Already in 1975 Bathurst [28] suggested that the growth of a stylolite could stop when the permeability in the adjacent sediment has fallen so low that transport of ions away from the solution film is practically inhibited. The role of stylolites as a local source for cement is well accepted [7, 29-32], but how much of the dissolved material precipitates locally and how much is transported out of the system depends on local conditions and their temporal evolution. The frequency of open fractures and their connectivity as well as permeability of the bulk control how "open" or "closed" the system is. Thin-sections of the Blanche show that current porosity is close to zero both close to the stylolites and at mid-points between adjacent stylolites and that the initial porosity is filled by cement. Very few small fractures or veins were identified, which also supports the concept of a closed system in which pore fluid has no path out and precipitation occurs near-by. Thus we suggest that the life cycle of stylolites in our case-study was controlled by precipitation: once pore space was completely cemented – the process of stylolitization stopped.

5.2 The correlation length – measured for the first time

In the present work we measured for the first time the upper bound of self-affinity and the correlation length which were predicted by previous theoretical studies [1, 2, 10, 11, 14]. Karcz and Scholz [13] analyzed roughness of stylolites from several field sites on 2D traces and found them to be self-similar from scales of 10 microns to 2.5m. They found one regime with H=0.55. Other previous studies [10, 11, 13, 14] showed fractal stylolite roughness over several orders of magnitude, up to ~10cm. These studies showed two self-affine regimes for scales smaller and larger than ~1.1mm, with roughness exponents of H_S~1.1 (for small scales) and H_L~0.5 (for large scales). The authors

connected this to two competing mechanisms driving dissolution: surface energy and elastic strain energy. The larger scales they measure correlate to the smaller scales in our LIDAR measurements, and the part with H~1.1 is below our resolution. The two regimes discussed in these papers, are therefore **not** the two regimes we present, and the correlation length was not measured in these cases either.

These previous stylolite roughness measurements have not measured the upper bound to fractality before, either because the largest scale of measurement was smaller than the correlation length, or because the correlation length had reached the system size. When stylolites are connected by a framework of fractures (such as in the case of Karcz and Scholz [13]), it may indicate that the system was open, at least to some degree, thus allowing dissolution to continue and roughness to develop to very large correlation lengths. In such a case, it would require very large sampling size to capture χ, or χ may even have reached the system size.

An alternative explanation to why the upper cutoff to fractality has not been reported by others is that not all stylolites are formed from existing flat surfaces, as the Blanche stylolites. Other types of stylolite populations have been reported in the literature, as summarized in [8]. For different types of stylolites roughness develops differently, especially for those which propagate laterally. Their roughness is expected to be more developed in the center and decrease towards the "younger" stylolite edges, as observed by Stockdale [6].

5.3 Upper bound to fractality: is it a good measure for A?

Estimates of amount of dissolution on stylolites have been performed by various authors (e.g.: [3, 5, 33, 34]). The common methods used are summarized in table 1 of Tada and Seiver [7]. These include maximum teeth amplitude, seam thickness, heavy mineral condensation, displacement of veins and reconstruction of fossils and oolites. We have presented here an additional method for estimating the amount of dissolution and found that its results are comparable (similar order of magnitude) to maximum teeth amplitude and to mass balance calculations. The common method used for evaluating

amount of dissolution from cores is by measuring the maximum amplitude. Two issues should be discussed:

1. When is maximum amplitude, A_{max}, a good measure of dissolution amount?

The answer to this question is that A_{max} is a good measure of dissolution in case the sampling size is larger than the correlation length. If it is smaller it will probably give an underestimate. For example, if we measure A_{max} for $l=\chi/2$ (assuming $A_{max}(\chi/2)/A_{max}(\chi) = w(\chi/2)/w(\chi)$, [20]), the dissolution underestimation would be, from equation (7): $\frac{A_{\max(\chi/2)}}{A_{\max(\chi)}} = \frac{\left(\frac{(\chi/2)^H}{a}\right)^{\frac{Z}{H}} a}{\left(\frac{(\chi)^H}{a}\right)^{\frac{Z}{H}} a} = 2^{-Z}$. For z=1 the value of measured A_{max} will be 0.5 of the value measured when $l=\chi$. In general, the underestimated value would be b^{-z} for measurement size $l=\chi/b$.

Another requirement for A_{max} to be a good measure of the dissolution amount is that the measured stylolite evolved on a pre-existing surface. If it evolved from a seed and grew laterally, the position from where the sample is taken is expected to have major influence on roughness. It is unknown at this stage how such different stylolite groups can be differentiated when studied in a core, but this is one interesting question to investigate in the future.

2. Is dissolution amount based on roughness measurements a better estimate than other methods?

The answer to this question is currently no. The main reason is that the major parameter which is unknown and evaluated only from models is the dynamic exponent, z. This parameter defines the time-dependence of the evolution of roughness. In our calculation we gave a lower and upper estimate of this parameter, which resulted in quite a large range for A (between 10 and 70cm). This parameter could be better constrained from field studies of stylolitization evolution with time, or from laboratory experiments but these are obviously not easy to conduct, as stylolites have never been produced in the lab (except on the sub-grain scale by [35]).

6 Summary and conclusions

In this paper we have presented 3D roughness measurements of stylolite surfaces at a scale larger than ever measured before. We have compared these measurements to predictions from a model of surface roughening from an initially flat interface. The six analyzed surfaces show self affine characteristics with H of 0.67 ±0.10 for scales of several mm and up to ~10cm. Above this scale, H decreases almost to zero, indicating that there is an upper cutoff to the self-affine behavior of these stylolite surfaces. The existence of this upper cutoff, termed the "correlation length" (χ), was interpreted as an indicator that the stylolitization process stopped before roughness has saturated. We proposed a scenario in which dissolution and hence roughening stopped when all available porosity around the stylolites was shut down by precipitation originating from the material dissolved on the stylolites. A method for estimating the amount of dissolution, on stylolites from their roughness characteristics in cases where χ is much smaller than the stylolites length was presented. Dissolution amount for the Blanche stylolites was calculated and compared to its estimates from two other methods. The agreement between the three independent methods indicates that the upper bound to fractality of stylolites' roughness can indeed indicate on the amount of dissolution. One very important implication of the agreement between the models and measurements is that it provides support for formation of stylolites, at least in this field site, from existing surfaces. These surfaces could be perhaps of higher clay content [8]. This is in contrast to in-plane propagation of stylolites, as suggested for other cases (e.g. [8, 36, 37]).

Reference List

1 M. Ebner, D. Koehn, R. Toussaint, F. Renard and J. Schmittbuhl, Stress sensitivity of stylolite morphology, Earth and Planetary Science Letters 277(3-4), 394-398, 2009.

2 D. Koehn, F. Renard, R. Toussaint and C.W. Passchier, Growth of stylolite teeth patterns depending on normal stress and finite compaction, Earth and Planetary Science Letters 257(3-4), 582-595, 2007.

2bis Modeling the growth of stylolites in sedimentary rocks.
Rolland A., R. Toussaint, P. Baud, J. Schmittbuhl, N. Conil, D. Koehn, F. Renard, J.P. Gratier, submitted to J. Geoph Res.

3 M.T. Heald, Stylolite in sandstones, The Journal og Geology 63(2), 101-114, 1955.

4 W.C. Park and E.H. Schot, Stylolites - Their Nature and Origin, Journal of Sedimentary Petrology 38(1), 175-&, 1968.

5 M.Y. Kaplan, Origin of stylolites, Docl. Acad. Sci USSR, Earth Sci. Sect. 221, 205-7, 1976.

6 P.B. Stockdale, Stylolites: their nature and origin, Indiana University Studies 9, 1-97, 1922.

7 R. Tada and R. Siever, Pressure Solution During Diagenesis, Annual Review of Earth and Planetary Sciences 17, 89-118, 1989.

8 L. Laronne Ben-Itzhak, R. Katsman, A. E., Z. Karcz and M. Kaduri, Stylolite Populations in Limestone: Field Observations and Formation Models, Journal of Geophysical Research -Solid Earth, submitted.

9 Z. Karcz, E. Aharonov, D. Ertas, R. Polizzotti and C.H. Scholz, Stability of a sodium chloride indenter contact undergoing pressure solution, Geology 34(1), 61-63, 2006.

10 F. Renard, J. Schmittbuhl, J.P. Gratier, P. Meakin and E. Merino, Three-dimensional roughness of stylolites in limestones, Journal of Geophysical Research-Solid Earth 109(B3), -, 2004.

11 J. Schmittbuhl, F. Renard, J.P. Gratier and R. Toussaint, Roughness of stylolites: Implications of 3D high resolution topography measurements, Physical Review Letters 93(23), -, 2004.

12 B.B. Mandelbrot, Fractals in Physics, Elsevier, Amsterdam, 1986.

13 Z. Karcz and C.H. Scholz, The fractal geometry of some stylolites from the Calcare Massiccio Formation, Italy, Journal of Structural Geology 25(8), 1301-1316, 2003.

14 M. Ebner, D. Koehn, R. Toussaint and F. Renard, The influence of rock heterogeneity on the scaling properties of simulated and natural stylolites, Journal of Structural Geology 31(1), 72-82, 2009.

15 M. Safaricz, Pressure solution in chalk., Ph.D., Royal Holloway University of London., 2002.

16 M. Safaricz and I. Davison, Pressure solution in chalk, Aapg Bulletin 89(3), 383-401, 2005.

17 E. Aharonov and R. Katsman, Interaction between Pressure Solution and Clays in Stylolite Development: Insights from Modeling, American Journal of Science 309(7), 607-632, 2009.
18 A. Sneh and R. Weinberger, Geological Map of Israel. Sheet 2-II Metulla, Israel Geological Survey, 2003.
19 E.J. Oswald, H.W. Mueller III, D.F. Goff, H. Al-Habshi and S. Al-Matroushi Adco, Controls on Porosity Evolution n Thamama Group Carbonate Reservoirs in Abu Dhabi, U.A.E, Middle East Oil Show, 251-265, 1995.
20 J. Schmittbuhl, F. Schmitt and C. Scholz, Scaling Invariance of Crack Surfaces, Journal of Geophysical Research-Solid Earth 100(B4), 5953-5973, 1995.
21 A.L. Barabasi and E.H. Stanley, Fractal concepts in surface growth, Cambridge Univ. Press, New York, 1995.
22 A. Sagy and E.E. Brodsky, Geometric and rheological asperities in an exposed fault zone, Journal of Geophysical Research-Solid Earth 114(B02301), 15 PP, 2009.
23 F. Family and T. Viscek, Scaling of the active zone in the Eden process on percolation networks and the ballistic depositional model, Journal of Physics A: Mathematical and General 18(2), 1985.
24 J. Schmittbuhl, S. Roux, J.P. Vilotte and K.J. Maloy, Interfacial Crack Pinning: Effect of Nonlocal Interactions, Physical Review Letters 74(10), 1787-1790, 1995.
25 J. Schmittbuhl, A. Steyer, L. Jouniaux and R. Toussaint, Fracture morphology and viscous transport, International Journal of Rock Mechanics and Mining Sciences 45(3), 422-430, 2008.
26 S. Santucci, M. Grob, R. Toussaint, J. Schmittbuhl, A. Hansen and K.J. Maloy, Fracture roughness scaling: A case study on planar cracks, Epl 92(4), -, 2010.
27 I. Simonsen, D. Vandembroucq and S. Roux, Wave scattering from self-affine surfaces, Physical Review E 61(5), 5914-5917, 2000.
28 R.G.C. Bathurst, Carbonate sediments and their diagenesis, 658 pp., Elsevier, Amsterdam, 1975.
29 P.K. Wong and A. Oldershaw, Burial Cementation in the Devonian, Kaybob Reef Complex, Alberta, Canada, Journal of Sedimentary Petrology 51(2), 507-520, 1981.
30 O. Walderhaug and P.A. Bjorkum, The effect of stylolite spacing on quartz cementation in the Lower Jurassic Sto Formation, southern Barents Sea, Journal of Sedimentary Research 73(2), 146-156, 2003.
31 S.N. Ehrenberg, Porosity destruction in carbonate platforms, Journal of Petroleum Geology 29(1), 41-51, 2006.
32 E.A. Finkel and B.H. Wilkinson, Stylolitization as Source of Cement in Mississippian Salem Limestone, West-Central Indiana, Aapg Bulletin-American Association of Petroleum Geologists 74(2), 174-186, 1990.
33 P.B. Stockdale, The stratigraphic significance of solution in rocks, Journal of Geology 34, 399-414, 1926.

34 D.F. Sibley and H. Blatt, Intergranular Pressure Solution and Cementation of Tuscarora Orthoquartzite, Journal of Sedimentary Petrology 46(4), 881-896, 1976.
35 J.P. Gratier, L. Muquet, R. Hassani and F. Renard, Experimental microstylolites in quartz and modeled application to natural stylolitic structures, Journal of Structural Geology 27(1), 89-100, 2005.
36 S. Raynaud and E. Carrioschaffhauser, Rock Matrix Structures in a Zone Influenced by a Stylolite, Journal of Structural Geology 14(8-9), 973-980, 1992.
37 R.C. Fletcher and D.D. Pollard, Anti-Crack Model for Pressure Solution Surfaces, Geology 9(9), 419-424, 1981.

Tables

Table 1: Physical and statistical characteristics of six stylolite surfaces from the Blanche cliff, Northern Israel. Hurst exponents calculated using three independent methods are shaded in blue (RMS= root mean square; PSD=power spectral density). H is significantly different below and above χ, the correlation length. χ and w(χ) are yellow-shaded; *a* (characteristic size calculated by equation 6) and A (amount of dissolution) are green-shaded. z is the dynamic exponent, as explained in section 3. The last row shows average values of each column and its standard deviation.

#	Sample Name	Dimensions (m)		H, $l<\chi$			H, $l>\chi$		χ (m)	w(χ) (m)	*a* (μm)	A (m)	
		length	width	RMS	PSD	wavelet	RMS	PSD				z=1.2	z=1.0
1	*in situ* 1	2.14	0.20	0.57	0.5	0.56	0.04	0.02	0.12	0.0050	74	0.53	0.12
2	*in situ* 2	9.32	0.30	0.72	0.67	-	0.15	0.2	0.07	0.0040	5	0.47	0.07
3	*in situ* 3	4.80	0.12	0.63	0.68	-	0.11	0.11	0.08	0.0047	1	0.84	0.08
4	*in situ* 4	3.30	0.23	0.75	0.82	0.8	0.02	-0.24	0.11	0.0050	26	0.58	0.11
5	rockfall 1	5.37	2.73	0.64	0.67	-	0.11	0.16	0.11	0.0050	2	1.00	0.11
6	rockfall 2	2.50	2.14	0.7	0.79	0.62	0.15	0.18	0.11	0.0045	15	0.65	0.11
	Average (std)			**0.67 (0.07)**	**0.69 (0.11)**	**0.66 (0.12)**	**0.10 (0.06)**	**0.07 (0.16)**	**0.10 (0.02)**	**0.0047 (0.0004)**	**20 (28)**	**0.68 (0.20)**	**0.10 (0.02)**

Appendix

Parameters used in this manuscript, their symbols and units.

Symbol	***Name***	*Units*
A	Dissolution amount	m
L	Sampling size	m
L	System size	m
X	Correlation length	m
t_c	Critical time for which χ=L	s
W	Average "width" of stylolite interface	m
H	Hurst exponent	
Z	Dynamic exponent	
A	Characteristic size of the system	m
V	Dissolution rate	m/s
D	Spacing between stylolites	m
ϕ	Porosity	

Figure Captions

Figure 1: Photos of the study area: (a) Blanche cliff; (b) an exposed stylolite surface which was scanned using the LIDAR technique ("*in-situ* 1" in Table 1, long axis of surface is ~2 m); (c) cross-section view of 2 parallel stylolites (see camera cover for scale).

Figure 2: Topography of one of the scanned surfaces ("rockfall 1", in Table 1) after data interpolation to an xyz grid.

Figure 3: (a) RMS and (b) PSD analysis of surface roughness of 6 stylolite surfaces in the Blanche cliff (see Table 1 for dimensions and detailed results for each surface). The x-axis of the PSD analysis is k [m^{-1}], as costumed in the literature, and equals $(2*l)^{-1}$. Two scaling regimes are seen: (1) self-affine behavior with H~0.7 for scales up to l~10cm; and (2) decrease of slope (H decreases) at larger scales up to almost flattening (H~0.1). The range of values for which H starts decreasing, this is very soft definition …. is marked by grey rectangles and is between 7 and 12 cm. This value is the correlation length, χ, as explained in section 3.

Figure 4: Modified from Figure 2 of Ebner et al. [14]. Simplified sketch of the numerical model setup which simulates stylolite roughening from an initial flat interface (marked by a red line). Initial setup is seen in (a), while the configuration after a certain amount of compaction appears in (b). The darker spheres are "pinning particles" which have a lower solubility and drive roughening.

Figure 5: Simulation results, from Figure 4 of Koehn et al. [2] on which we added schematic illustration of how maximum amplitude, A_{max} depends on time and on sampling size, l. For example: maximum amplitude of l_2 at t_2 is smaller than at t_3. At a given time A_{max} depends on l up to a critical size, after which it remains constant (e.g.: for $l > l_2$, A_{max}=const). This dependence on l is a characteristic of self affine surfaces.

Figure 6: Schematic log-log plot of w(l) for several times according to roughening models of Ebner et al. [14] and Koehn et al. [2]. For each time there is a power-law dependence of w on l with an exponent H (dotted black line) up to $l=\chi$. χ increases with time until it reaches the system size, L (assuming the process has not stopped before). At χ=L (t=tc) roughness stops evolving though dissolution may still continue.

Figure 1:

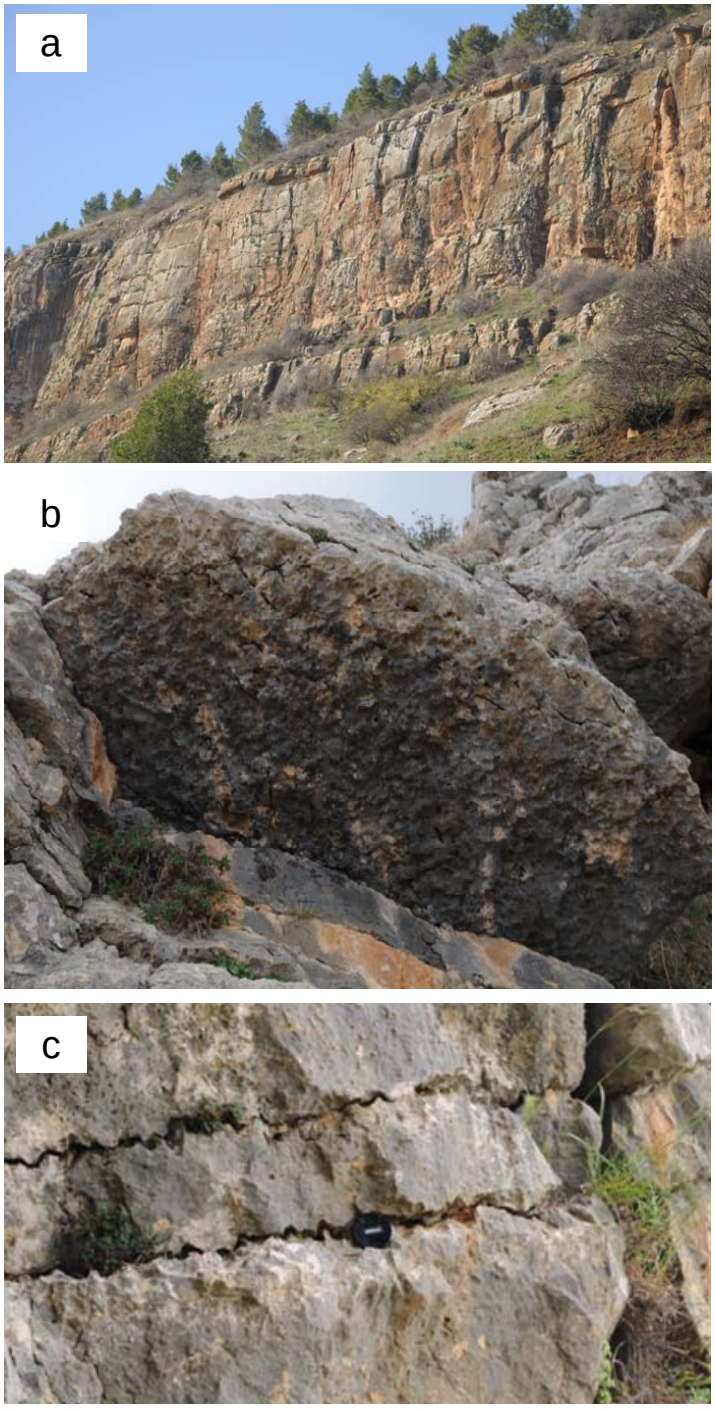

Figure 2:

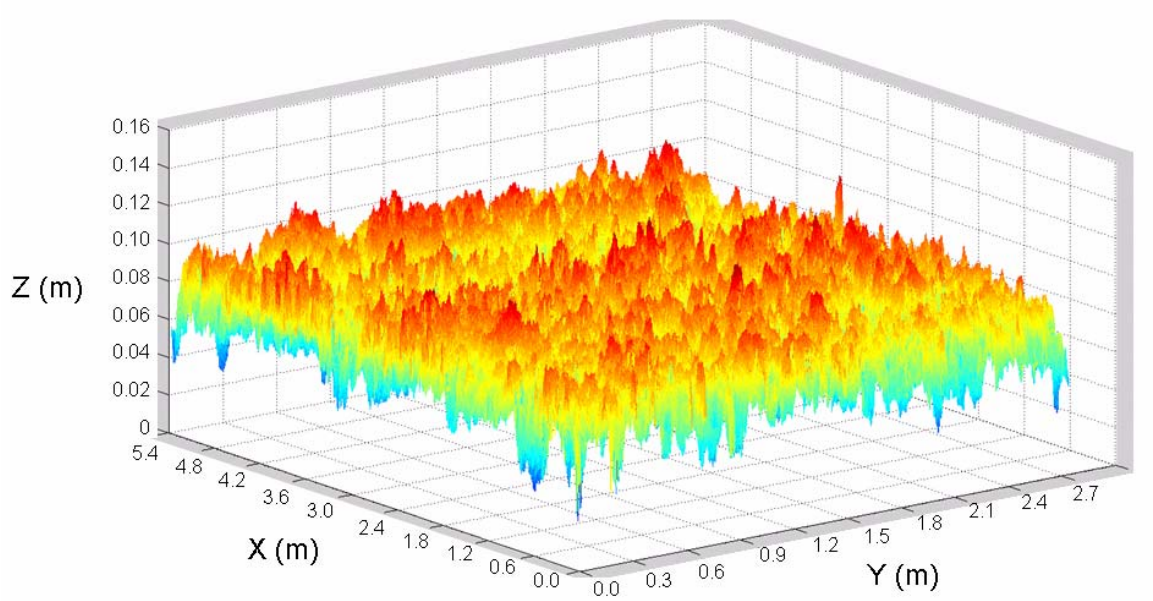
Z (m)
0.16
0.14
0.12
0.10
0.08
0.06
0.04
0.02
0
X (m)
5.4
4.8
4.2
3.6
3.0
2.4
1.8
1.2
0.6
0.0
Y (m)
0.0
0.3
0.6
0.9
1.2
1.5
1.8
2.1
2.4
2.7

Figure 3:

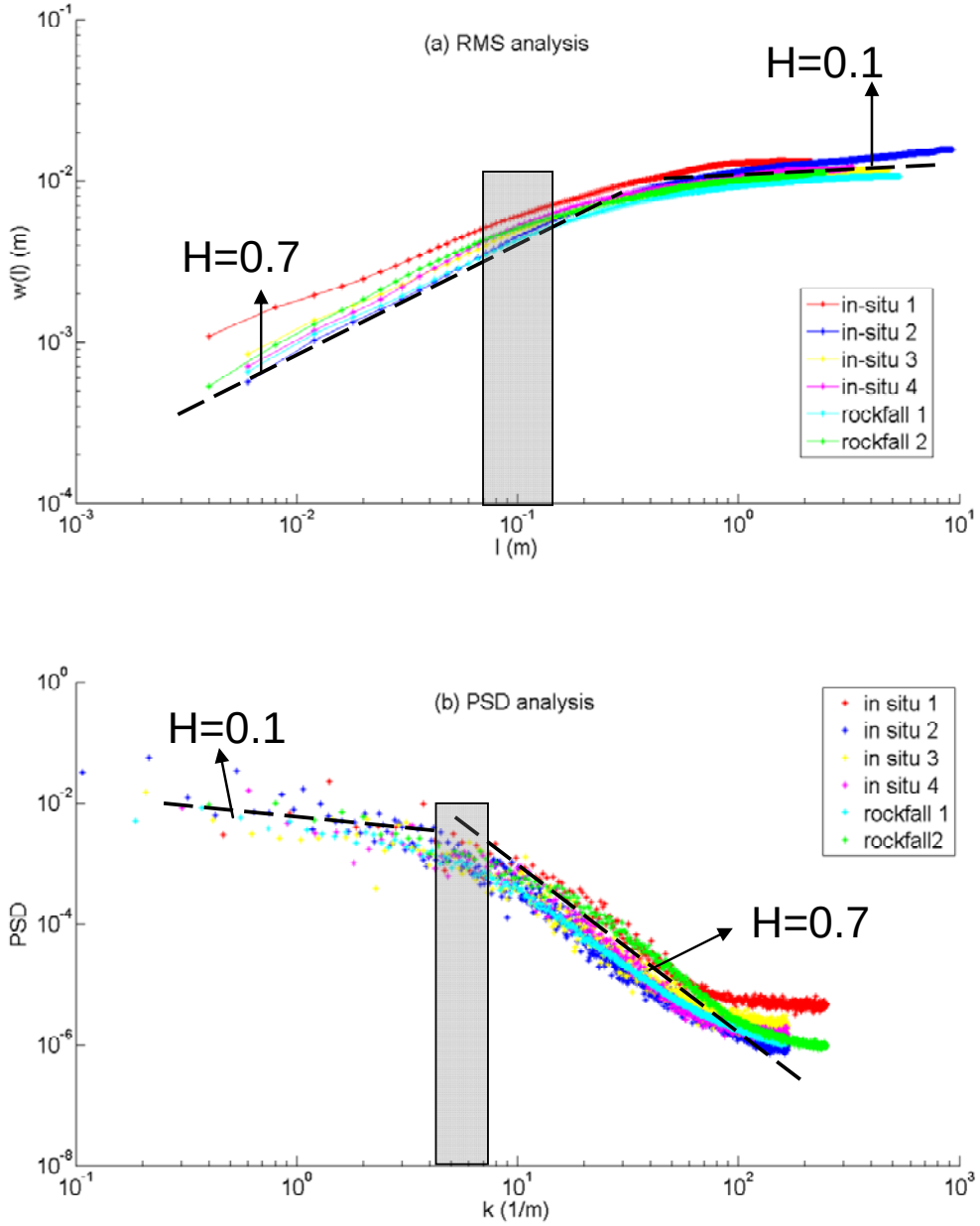
(a) RMS analysis
H=0.1
H=0.7
w(l) (m)
l (m)
in-situ 1
in-situ 2
in-situ 3
in-situ 4
rockfall 1
rockfall 2
(b) PSD analysis
H=0.1
H=0.7
PSD
k (1/m)
in situ 1
in situ 2
in situ 3
in situ 4
rockfall 1
rockfall2

Figure 4:

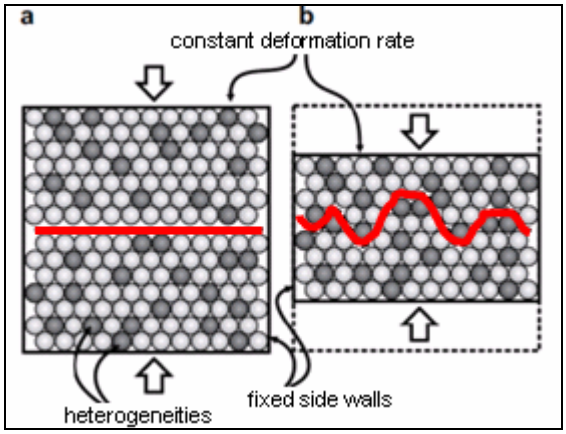
a
b
constant deformation rate
heterogeneities
fixed side walls

Figure 5:

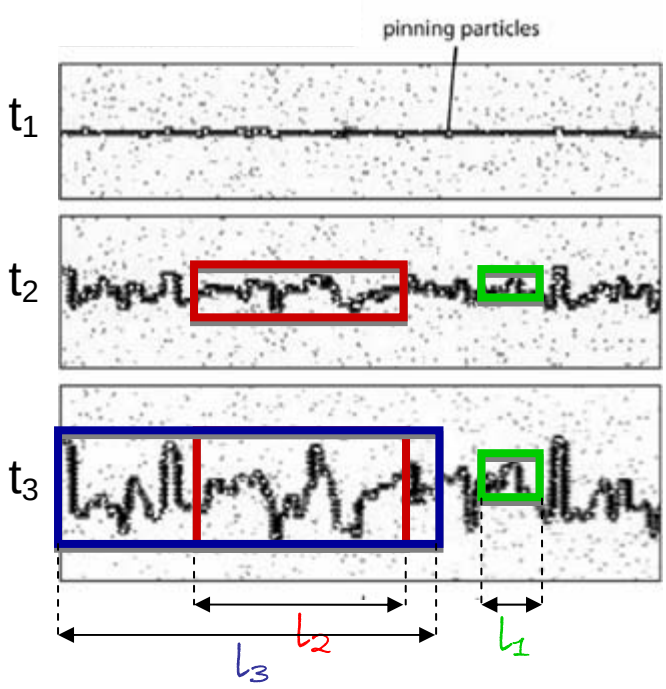

Figure 6: